

Long-term degradation study of Polytetrafluoroethylene in a low temperature oxygen plasma

Tobias Wagner, Marcus Rohnke*, Jürgen Janek*

Institute of Physical Chemistry and Center for Materials Research, Justus Liebig University Giessen, Heinrich-Buff-Ring 17, D 35392 Giessen, Germany

ARTICLE INFO

Keywords:

Low temperature oxygen plasma
Polymer degradation
Surface analysis
Degradation mechanism

ABSTRACT

Atomic oxygen (AO) is the most common gas species in the Low-Earth-Orbit (LEO) and responsible for material degradation of the outer shell of spacecrafts within this space region. Due to their similar properties, low temperature oxygen plasmas are suited for material degradation studies taking place on earth instead of quite expensive space studies. Here we focus on the long-term degradation of Polytetrafluoroethylene (PTFE), which is often employed on the outside of spacecrafts. Up to date, there is no complete understanding of the degradation process on molecular level, which is necessary for materials improvement and new materials development.

For the degradation studies, a self-constructed capacitively driven 13.56 MHz RF reactor was used to generate an oxygen plasma for the simulation of LEO conditions. PTFE was characterised in the pristine state and after AO treatment at different times by ToF-SIMS, XPS and SEM. During plasma treatment, the samples show a linear mass loss behaviour. ToF-SIMS surface analysis reveal mass fragments which show a clear chemical reaction of oxygen species with PTFE. The presence of these molecular indicators was verified by XPS, where additional carbon species were found after plasma treatment. SEM micrographs showed an inhomogeneous degradation on the surface in the first hours similar to actual LEO exposure. For a complete understanding of the degradation progress, operando mass spectrometric studies of the plasma composition were carried out to detect volatile degradation products.

In summary, a steady degradation has been observed that leads to constant mass loss, defluorination, chain shortening and insertion of oxygen into the polymer.

1. Introduction

The low-earth-orbit (LEO) plays a crucial role in modern space technology. Many satellites are operating within this region due to its proximity to the earth's surface. In contrast to other regions in space, the LEO has an atmosphere consisting mostly of atomic oxygen (AO), which is hazardous to most materials used in space applications. AO is mainly formed by solar UV photons below a wavelength of 243 nm breaking apart the molecular O₂ bond. Depending among other factors on the altitude and solar activity, a spacecraft traveling with a velocity of 8 km·s⁻¹ is exposed to a flux of 10¹⁴–10¹⁵ atoms of oxygen cm⁻²·s⁻¹ [1–3]. To simulate simplified LEO conditions, ground-based facilities are often used, utilizing oxygen plasmas to generate AO [4–7].

A material often used in space applications is polytetrafluoroethylene (PTFE), commonly known as Teflon [2,8]. Applications for PTFE in this context include space suits ("Beta cloth"), protective shields

for satellites and rockets as well as wire insulation. Similar to many other polymers, it is a lightweight material, which is a crucial property [9]. Furthermore, PTFE has proven to be much more resistant to AO than most other materials, showing an erosion yield of 1.42·10⁻²⁵ cm³·atom⁻¹, only [10]. The erosion yield is a material constant calculated from LEO flight experiments describing the volume loss per impacting oxygen atom. Due to the fluctuating conditions in the LEO, slightly different values have been reported from space flight experiments [11].

Many studies have investigated the changes PTFE undergoes after short AO treatment, often focusing on optical and mechanical properties [12–17]. Studies for long treatment times does not exist. Surface sensitive characterization methods, such as time-of-flight secondary ion mass spectrometry (ToF-SIMS) and x-ray photo emission spectroscopy (XPS), have also been employed in similar studies [18,19]. However, the potential of these methods has not yet been fully exploited. Valuable

Abbreviations: AO, atomic oxygen; PTFE, polytetrafluoroethylene; LEO, low-earth-orbit.

* Corresponding authors.

E-mail addresses: Marcus.Rohnke@pc.jlug.de (M. Rohnke), Juergen.Janek@pc.jlug.de (J. Janek).

<https://doi.org/10.1016/j.polymdegradstab.2024.110989>

Received 19 July 2024; Received in revised form 30 August 2024; Accepted 30 August 2024

Available online 31 August 2024

0141-3910/© 2024 The Author(s). Published by Elsevier Ltd. This is an open access article under the CC BY-NC license (<http://creativecommons.org/licenses/by-nc/4.0/>).

insights into ongoing degradation reactions can be obtained by the application of statistical tools for data evaluation. As shown in the literature, multivariate statistical methods such as principal component analysis (PCA) and multivariate curve resolution (MCR) can be used to evaluate SIMS data to gain a better understanding of the degradation mechanisms of different materials, including other polymers [20,21].

In the present work, we focus on the chemical surface analysis of PTFE samples before and after long-term oxygen plasma treatment. Scanning electron microscopy (SEM) was used to investigate the morphological changes during AO exposure. For a characterization of the chemical composition of the sample surface, ToF-SIMS analysis was carried out. To obtain more information from the mass spectra, multivariate statistical methods such as PCA and MCR were employed. While PCA is usually well known in the scientific community, MCR is often neglected. However, MCR can provide additional information, as it is designed specifically to solve the mixture analysis problem [22,23]. By this mean, spectra of mixtures are deconvoluted into a set of additive, and most importantly, chemically sensible spectra. Therefore, interpretation of MCR results can be more accessible than that of PCA results. Complementary to the SIMS measurements, XPS was used to validate these findings. Finally, operando quadrupole mass spectrometry (QMS) was used to obtain information on the changes occurring within the plasma composition during treatment. The obtained data was then subjected to multivariate statistical tools to gain further insight into the degradation process. This work aims to fully elucidate the degradation mechanism of PTFE in artificial space conditions.

2. Materials and methods

2.1. PTFE

A PTFE sheet (Merck – Sigma Aldrich) of 1 mm thickness was cut into samples of approximately $20 \times 20 \text{ mm}^2$. For mass loss experiments, the samples were then weighted on a precision balance and placed on the grounded electrode of the plasma chamber. After plasma treatment, the samples were weighted again, and the mass loss calculated. Furthermore, the geometry and exposed surface area of the samples were measured.

2.2. Oxygen plasma

The capacitive oxygen plasma was generated in an apparatus consisting of a PFG 300 RF-Generator (TRUMPF Hüttinger GmbH, Germany) connected to a stainless-steel electrode (9 cm diameter, placed horizontally) via a PFM 1500 A matchbox (TRUMPF Hüttinger GmbH, Germany). A stainless-steel grounded electrode (9 cm diameter) is 9 cm below the driven electrode. After evacuation to 0.1 mbar, the chamber was flushed with 5.0 oxygen to 1 mbar and then evacuated to 0.1 mbar again. This procedure was then repeated for cleaning once before the plasma was ignited at 0.1 mbar. A negative bias of 150 V was applied to the driven electrode while the power was regulated and remained at 10 W. The RF-generator operated at a frequency of 13.56 MHz. During the plasma treatment, oxygen was supplied to the plasma chamber at a rate of 0.025 sccm while a rotatory pump connected via a valve kept the pressure constant at 0.1 mbar (± 0.03 mbar). An image of the apparatus can be seen in the Supplementary Information (Figure S1).

2.3. Operando-QMS

To perform operando measurements in the plasma reactor, a PrismaPro QMG 250 quadrupole mass spectrometer from Pfeiffer Vacuum (Aslar, Germany) in combination with a turbomolecular pump were installed at a cross fitting via CF-40 flanges. The cross fitting was connected to the plasma chamber via a double-sided blind flange that was pierced by a capillary with a diameter of 5.5 mm and a length of 95 mm. This setup enabled the quadrupole mass spectrometer to operate in the

10^{-5} – 10^{-6} mbar pressure range without disturbing the plasma pressure. Mass spectra were recorded with a dwell time of 16 ms, 20 points- amu^{-1} , a range of 0–200 m/z , and an activated electron multiplier.

2.4. SEM

SEM images were acquired with a Merlin high-resolution SEM (Carl Zeiss AG, Oberkochen, Germany) at a pressure in the low 10^{-6} mbar range, a probing current of 90 pA, and an electron acceleration voltage of 3 kV. An in-lens secondary electron detector was used for image acquisition. To prevent charging effects, the insulating samples were coated with 4 nm of Pt using an EM ACE 600 sputter coater (Leica, Wetzlar, Germany).

2.5. XPS

A PHI 5000 VersaProbe 4 Scanning ESCA Microprobe (Physical Electronics, Chanhassen, USA) with monochromatized Al K_{α} X-ray source (beam diameter of 100 μm , X-ray power of 100 W) was used to measure XP spectra. An analyzer pass energy of 27 eV, a step time of 50 ms, and a step size of 0.05 eV were used for measuring detail spectra. During the measurements, charge neutralization with slow electrons was applied. CasaXPS software was used for data evaluation and the charge correction was applied using the CF signal in the F1s (689.4 eV) spectrum as reference. For all fitted signals, a Shirley background was used.

2.6. ToF-SIMS

ToF-SIMS measurements were carried out with a M6 Hybrid-SIMS instrument (IONTOF GmbH, Münster, Germany), equipped with a 30 kV Bi cluster primary ion gun (Nanoprobe 50) for analysis and a 20 keV gas cluster ion beam (GCIB) for depth profiling. All measurements were carried out with electron neutralization of the low energetic flood gun. For additional neutralisation, the pressure inside the analysis chamber was increased to $5 \cdot 10^{-6}$ mbar Ar. A surface potential of +440 V was used for all measurements. Surface analysis and depth profiling were carried out in spectrometry mode with Bi_3^{++} as primary ions (FWHM $m/\Delta m > 5000$ @ $m/z = 15.99$ (O^-)). The cycle time was set to 140 μs . An area of 100×100 (μm)² was analyzed with a 64×64 pixel field in random raster mode. For spectra, the stop condition was set to a primary ion dose of 10^{13} ions/ cm^2 . For depth profiling, Ar_{2000}^+ clusters (250×250 (μm)², 10 kV, 10.76 nA) were used as sputter species. After 1 sputter frame with 2 s pause time, 1 analysis frame with 1 shot/frame and 64×64 pixels was recorded. The stop condition was set to 300 scans. For all measurements, negative polarity was used.

2.7. AFM-SIMS

Surface roughness measurements and sputter yield measurements were carried out with a M6 Plus instrument (IONTOF GmbH, Münster, Germany), equipped with a Gas Cluster Ion Beam for depth profiling and an integrated atomic force microscope (AFM). Depth profiles were carried out with the same conditions as in the M6 Hybrid SIMS machine. For calculation of the sputter yield line scans were measured in tapping mode® before and after depth profiling. The erosion yield was calculated to $44 \text{ nm}^3/\text{Ar-cluster}$ and used for depth calibration of all depth profiles.

All SIMS data were evaluated with SurfaceLab 7.3 (IONTOF GmbH).

3. Results and discussion

3.1. Mass loss

To compare the plasma setup with LEO experiments, mass loss experiments were conducted. The change in mass was normalized to the

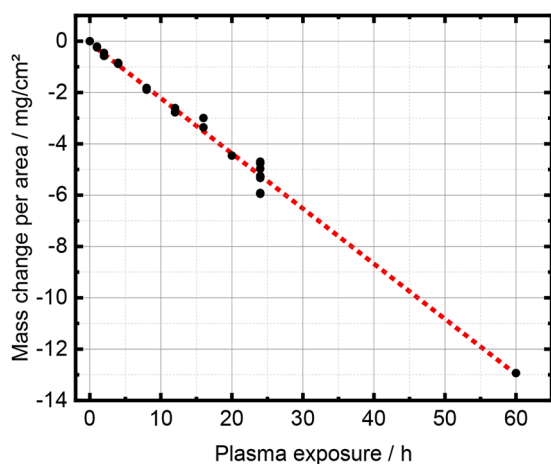


Fig. 1. Observed change in weight of PTFE samples after different plasma treatment times at 0.1 mbar, 150 V, 10 W, normalized to the exposed surface area. A linear change in mass can be observed.

exposed surface area of the samples. As can be seen in Fig. 1, the mass loss is linear even for long-term plasma exposure, indicating a steady degradation kinetics and no significant change in the degradation mechanism throughout the exposure.

From a linear fit with a R^2 of 0.989, a mass loss rate γ of $5.99 \cdot 10^{-8} \pm 0.15 \cdot 10^{-8} \text{ g} \cdot \text{cm}^{-2} \cdot \text{s}^{-1}$ was calculated.

The volume degradation Γ can be calculated according to Eq. (1):

$$\Gamma = \gamma / \rho \quad (1)$$

Where Γ = volume degradation ρ = density ($2.15 \text{ g} \cdot \text{cm}^{-3}$) [2]

In a next step, the flux of atomic oxygen in the plasma chamber towards the sample surface f_{PC} can be approximated according to formula (2). Here we use an erosion yield that was determined from experiments conducted in the LEO:

$$f_{\text{PC}} = \Gamma / E_s \quad (2)$$

Where f_{PC} = flux of atomic oxygen in the plasma chamber E_s = erosion yield ($1.42 \cdot 10^{-25} \text{ cm}^3 \cdot \text{atom}^{-1}$) [2].

For this setup, the flux of atomic oxygen f_{PC} was calculated to be approximately $2.0 \cdot 10^{17} \text{ atoms} / \text{cm}^2 / \text{s}$, three orders of magnitude higher than the flux in the LEO [2]. This allows long-term LEO exposure to be simulated in a much shorter time frame. In general, the question arises

what is the additional impact on degradation by typical plasma wall interactions. To rule out degradation effects induced by the plasma itself, reference experiments with an argon plasma were conducted. In contrast to oxygen plasma degradation for short exposure times ($<24 \text{ h}$) the mass loss was less than the sensitivity of the scale used (0.1 mg) and a degradation rate could not be calculated. After 24 h a mass loss of $0.2 \text{ mg} / \text{cm}^2$ was calculated (Figure S2). From this, it can be estimated that the degradation rate is more than two orders of magnitude lower than in an oxygen plasma, indicating that the chemical reaction of oxygen with the sample was mainly responsible for the degradation.

Low temperature plasma discharges are non-equilibrium systems consisting of anions, cations, electrons and neutrals [24]. Whereas charged particles can take up energy from the electric field and cause in the case of heavy ions sputter damage during plasma-wall interactions, the energy of neutrals is close to room temperature and they should not contribute to physical degradation. In order to ensure that plasma generated high energetic positively charged species did not impact the sample surface, a DC-Bias was applied to accelerate them to the driven electrode instead. In general, the concentration of negatively charged species - with exception of electrons - is negligible in low temperature discharges. Electrons can reach energies of up to 10.000 K but have negligible momentum due to their small mass and cause little sputter effects. In contrast to oxygen discharges pure argon plasmas do not contain any reactive neutral species. For the reasons mentioned, the degradation observed for the oxygen plasma treatment can be mainly attributed to neutral species, such as, AO.

3.2. SEM

In Fig. 2, SEM images of PTFE surfaces after different periods of plasma treatment are shown. On the pristine PTFE sample (a), the presence of cracks in the surface on a nm scale is obvious. After 2 h (b), erosion is clearly visible around plateau-like structures. The cracks are still present on the plateaus of this sample and remain seemingly unaltered, indicating that they are not starting points for degradation. This suggests a degradation that is independent of the nanostructure at the initial polymer surface. After 4 h (c), most of the surface is covered with craters with few plateaus in between. With longer plasma treatment times (d), no more plateaus can be observed. Additionally, there is no further change in the topography of the surface between samples that were treated for $>4 \text{ h}$. This indicates that the degradation at the surface is transitioning to a quasi-equilibrium, where, even though degraded material is steadily ablated from the sample, the bulk material serves as

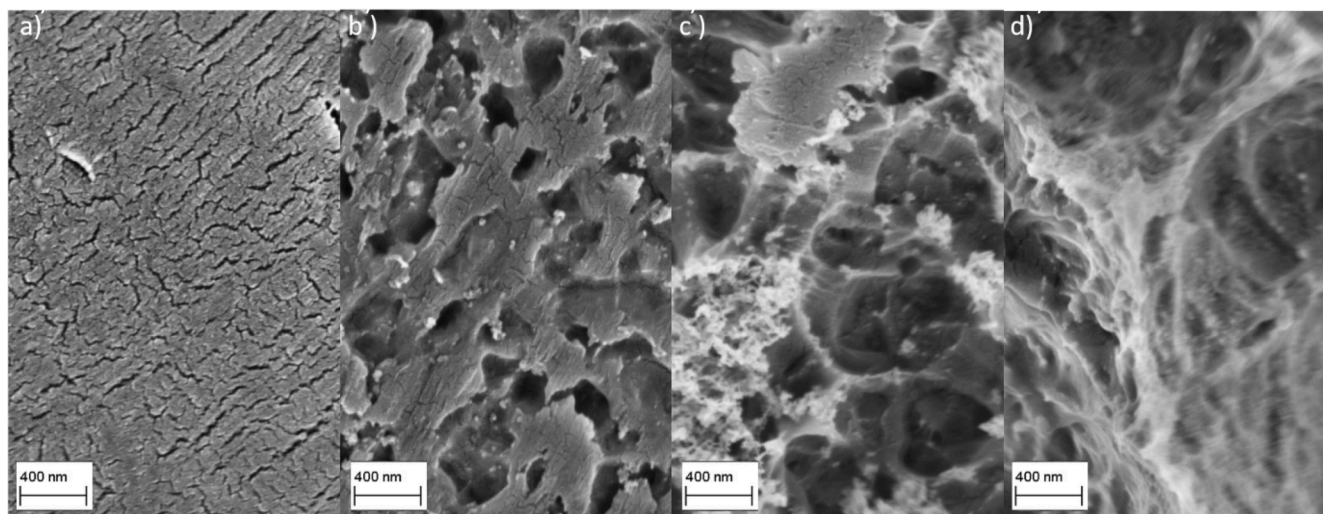


Fig. 2. Micrographs of samples treated for 0 h (a), 2 h (b), 4 h (c) and 12 h (d) in the oxygen plasma at 0.1 mbar, 150 V, 10 W. Increasing erosion of the surface with longer oxygen plasma treatment times can be observed.

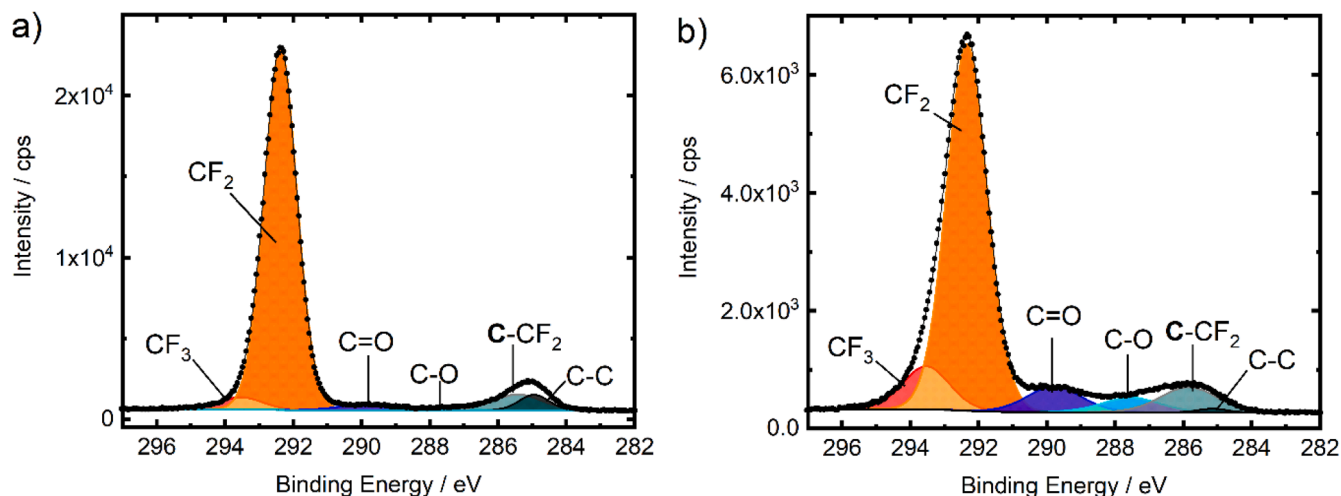


Fig. 3. C 1 s detail spectra from XPS measurements of an untreated (a) and a 2 h oxygen plasma treated (b) PTFE sample. Experimental conditions were 0.1 mbar, 150 V, 10 W. Recorded Datapoints are shown as dots, the outline as a black line. An increase in oxygenated and terminated carbon atoms can be observed.

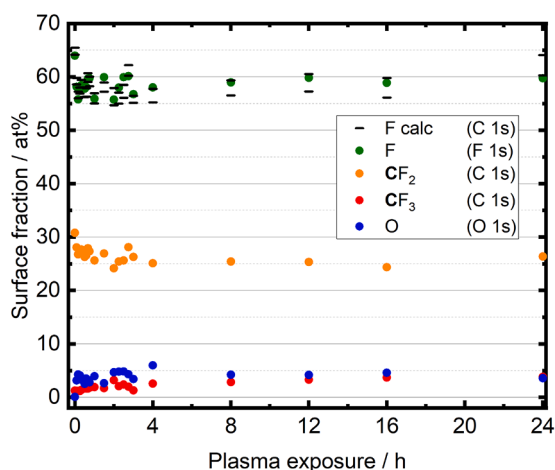


Fig. 4. Quantification results of XPS measurements on untreated ($t = 0$ h) and oxygen plasma treated PTFE samples. Starting with short plasma treatments (5 min), a decrease in fluorine content, as well as an increase in oxygen and terminated carbon content is visible.

an infinite reservoir of pristine PTFE. SEM micrographs of reference samples exposed to an argon plasma showed much less degradation at the sample surface (Figure S3).

3.3. XPS

In the C 1 s XPS detail spectra of an untreated (Fig. 3a) and a 2 h oxygen plasma treated sample (b), several signals can be observed. The most prominent peak in both spectra is the peak at 292.3 ± 0.1 eV, corresponding to CF_2 . A smaller peak at 293.5 ± 0.1 eV can be assigned to terminated carbon chains. After plasma treatment, this signal increases in intensity relative to the main signal. Furthermore, two signals likely belonging to oxidized carbon species appear at 289.8 ± 0.1 eV and 287.5 ± 0.1 eV respectively. At lower binding energies, two further signals that were interpreted as unfluorinated and unoxidized carbon can be fitted. These peaks are located at 285.7 ± 0.1 eV and 285.1 ± 0.1 eV respectively.

In Fig. 4, the quantification results from C 1 s, F 1 s and O 1 s fits are shown. The quantification on the reference sample ($t = 0$ h) closely matches the theoretical values of 67 % fluorine and 33 % carbon in PTFE. Additionally, a theoretical fluorine content was calculated for all samples from the respective CF_2 and CF_3 C 1 s signals according to Formula (3):

$$F_{\text{calc, lower limit}} = 2 \cdot \text{CF}_2 + 2 \cdot \text{CF}_3 \quad F_{\text{calc, upper limit}} = 2 \cdot \text{CF}_2 + 3 \cdot \text{CF}_3(3)$$

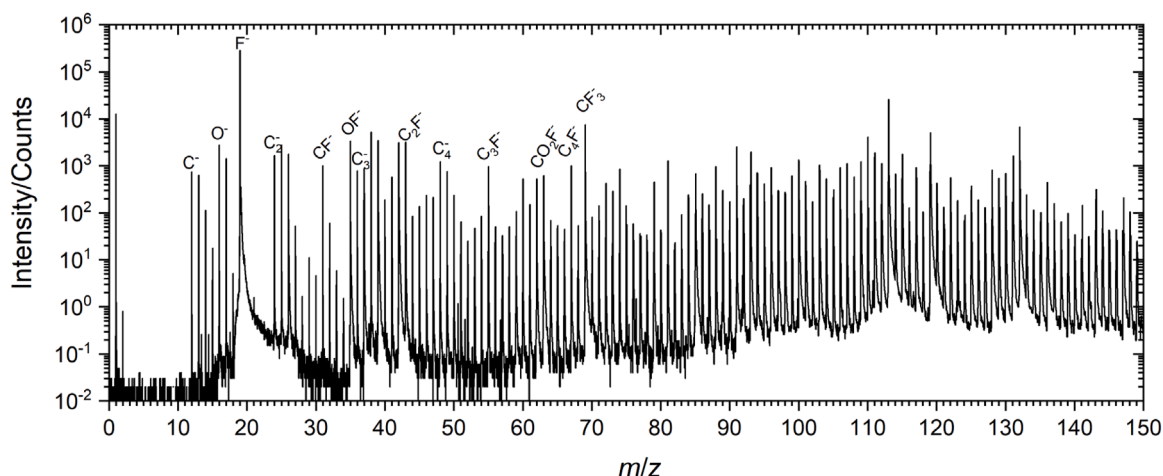


Fig. 5. Exemplary secondary ion mass spectrum in negative ion mode of a plasma treated ($t = 4$ h) PTFE sample surface.

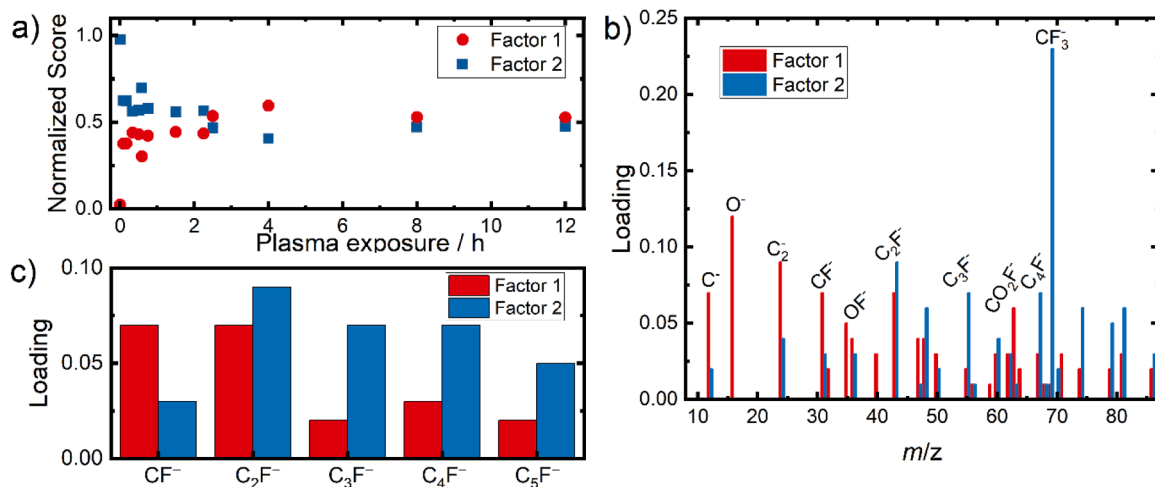


Fig. 6. Normalized Scores (a) and Loadings (b) obtained from a MCR with two factors applied to negative ion mode ToF-SIMS surface spectra of untreated ($t = 0$ h) and oxygen plasma treated PTFE samples. Factor 1 represents degradation products on the sample, whereas factor 2 corresponds to pure PTFE. Loadings of selected C_xF^- signals from the same MCR are shown in (c) to investigate a change in average chain length.

The lower limit was chosen to account for terminated and partially oxidized carbon (COF_2), which was assumed to appear during plasma treatment, whereas the upper limit accounts for only fully fluorinated carbon atoms (CF_3). As can be seen, the measured fluorine contents are indeed within these calculated limits. Generally, a trend can be observed where F 1 s content decreases during plasma treatment from 64 % to 56 %. As the observed values for fluorine content closely match the calculated values, carbon atoms inside the chain are likely either fully fluorinated or completely stripped of fluorine, as is evident from the presence of oxidized C 1 s species ($C = O$, $C-O$) after treatment. These signals increase from 1 % to 3.5 % and from <1 % to 2 % respectively. At the same time, an increase in oxygen content (O 1s: 0.5 to 4 %) is noted. Whereas CF_2 C 1 s decreases from 31 % to 25 %, the amount of CF_3 C 1 s increases from 1 % to 2 %, suggesting a higher presence of terminated carbon chains and therefore a shorter average chain length, resulting from degradation of the material. The composition of longer-treated samples does not change significantly. Elements other than carbon, oxygen and fluorine were not detected on any sample (Figure S4).

3.4. ToF-SIMS

Mass spectra generated from ToF-SIMS measurements, such as the one in Fig. 5, are usually quite complex and contain a lot of information.

To obtain a better understanding of the differences between the mass spectra of plasma treated and untreated samples, both principal component analysis (PCA) and multivariate curve resolution (MCR) were applied.

A PCA on mass spectra of samples treated in the plasma up to 24 h revealed two principal components (PCs) to account for 98 % of variance. Therefore, a follow-up MCR was employed with two factors, the results of which can be seen in Fig. 6. The normalized scores of factors 1 and 2, plotted against the oxygen plasma treatment times, are shown in a). The score of factor 1 is neglectable on the reference sample without plasma treatment ($t = 0$ h), but shows normalized scores of >0.3 on all plasma treated samples. After plasma treatment, the normalized score of factor 1 increases until 4 h treatment time, where a maximum value of 0.59 is reached. For longer plasma treatments, the score of factor 1 decreases slightly, but remains above 0.5. The loadings of factor 1 contain oxidized fragments, such as O^- , OF^- , and CO_2F^- , which clearly suggests that this factor can be assigned to the degradation products. Interestingly, C_2^- is also present in factor 1, further hinting at defluorination of some carbon atoms during treatment. The normalized score of factor 2 of 0.98 on the reference sample indicates that factor 2 represents the mass spectrum of pure PTFE. As can be seen from the loading plot in Fig. 6(b), factor 2 consists mainly of CF_3 , with other $C_xF_y^-$ fragments also present, similar to an expected mass spectrum of pure PTFE. It should be

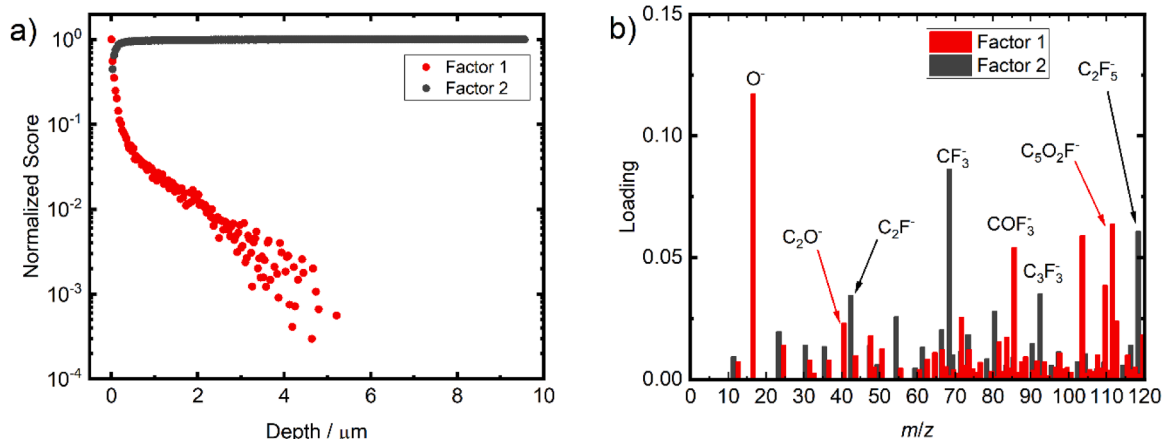


Fig. 7. Normalized scores (a) and loadings (b) obtained from a MCR with two factors applied to negative ion mode ToF-SIMS depth spectra of an oxygen plasma treated ($t = 4$ h) PTFE sample. Factor 1 is only present at the surface of the sample and represents degradation products, as well as surface contaminations. Factor 2 appears in the bulk material and corresponds to pristine PTFE.

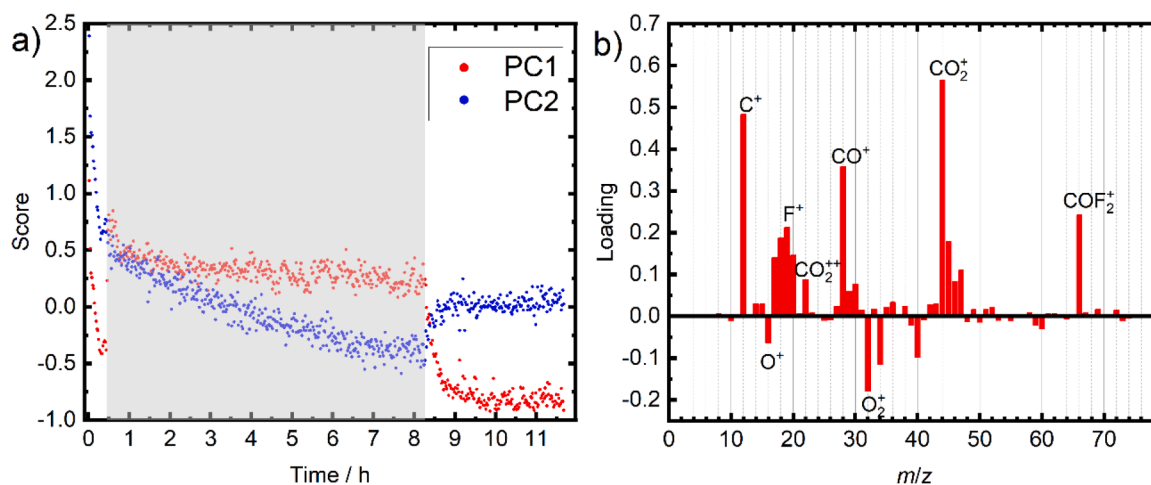


Fig. 8. Time dependent scores plot (a), as well as loading plot for PC1 (b) from the signal normalized PCA applied to operando mass spectra. Plasma treatment conditions were 0.1 mbar, 150 V, 10 W. The plasma treatment period is shown in grey. Positive loadings in b) correlate with plasma conditions, whereas negative loadings are associated with no plasma conditions.

noted here that surface contaminants, such as from handling the samples at air, are likely the same for all samples and thus have little impact on the loadings of factor 1.

The MCR loadings of selected C_nF^- mass signals with increasing carbon chain length (C_xF^- ; $x = 1, \dots, 5$) can be seen in c). The highest loading in factor 2 belongs to C_2F^- , with longer carbon chains also contributing significantly. In factor 1, shorter CF fragments are more relevant, with larger fragments having the lowest loadings. This again indicates the fragmentation of longer carbon chains into shorter ones during plasma treatment.

3.5. AFM/ToF-SIMS

From AFM-SIMS measurements, the surface roughness, as well as the depth calibration for the depth profiles were obtained.

MCR was also applied to data of SIMS depth profiles. As can be seen from the normalized scores against sputtering depth in Fig. 7(a), factor 1 represents the composition of the surface in contrast to the bulk material, which is present in factor 2. The loadings plot (b) for both factors reveals that oxygenated fragments, most importantly O^- , define factor 1, whereas factor 2 consists of unoxidized fragments from carbon and fluorine. These loadings are notably different from those obtained from surface spectra of different samples (Figure S5), as here surface contaminants play a large role in the difference between surface and bulk material. The normalized score of factor 1 decreases to about 0.01 at a nominal depth of 2 μm . This value however needs to be considered in combination with the surface roughness R_a of the sample, which is 0.9 μm . An AFM line scan of the sample is depicted in Figure S6. Therefore, at this nominal depth, it is likely that the score of factor 1 does not represent explicitly oxidation within the bulk material. Instead, it appears that due to the roughness, surface that had been exposed to and oxidized by the plasma was detected within the first μm due to shading effects during 3D analysis. No significant correlation between plasma treatment and either score of factor 1 or signal intensity of O^- at any given depth could be found. Thus, we conclude that the chemical degradation is mainly occurring at the exposed surface of the material, leaving the bulk mostly unaffected.

3.6. Operando-QMS

By conducting QMS measurements during the plasma treatment, additional insights into the degradation process can be acquired. Again, statistical methods were effectively employed to reveal the differences in the gas phase composition of the plasma reactor during and after

plasma treatment. A PCA of the received mass spectrometric data revealed that one principal component accounts for 99 % of variance. However, in this PCA only a few signals, such as O^+ and O_2^+ , accounted for the variance as these were expectedly the most prominent signals in the oxygen atmosphere of the plasma chamber. Further information was revealed by normalizing each mass signal on itself, specifically to the highest intensity of this signal in all measurement cycles. The results of this follow-up PCA can be seen in Fig. 8. Here, PC1 accounts for 22.3 % of variance, whereas PC2 explains 9.1 %. While the positive score of PC1 aligns very well with the presence of plasma conditions (a), the score of PC2 shows a constant trend downwards until the end of the plasma. Further PCs showed no correlation between score and time, likely a by-product of the normalization approach. This indicates that PC1 represents the variance introduced by the plasma. As can be seen in the loading plot for PC1 (b), most signals with a positive loading are carbon and oxidized carbon fragments (C^+ , CO^+ , CO_2^+). Other signals with less loading are fluorine containing species (F^+ , COF_2^+). Interestingly, no carbon species with only one fluorine atom attached could be observed. Pure oxygen species (O^+ , O_2^+) exhibit a negative loading, likely due to the reactions that oxygen undergoes in the plasma. Above a m/z ratio of 75, no further signal exhibited significant loading. The presence of degradation related carbon fragments in PC1 further supports the hypothesis of fragmentation of the polymer into shorter chains, as longer carbon chains were not observed.

4. Discussion

Even though oxygen plasmas are commonly used to simulate degradation in the LEO, there are still differences between the two. The atmosphere in LEO consists mainly of atomic oxygen, followed by either N_2 or He, depending on the altitude. While atomic oxygen is also abundant in plasmas comparable to the one used in this study, such a plasma atmosphere also contains atomic and molecular oxygen ions, mostly cations [4]. These cations are prevented from reacting with the sample by the DC-Bias, which accelerates them towards the driven electrode, away from the sample. This may introduce a sputter-deposition like process, with the electrode serving as the target. XPS spectra revealed no observable amount of metal on any sample, indicating that this effect is, if present at all, neglectable. Other sources of degradation present in LEO, which may have synergistic effects on the oxygen-based degradation, such as UV-radiation, debris impact or cosmic radiation, were also not considered in this study.

The combined results of SEM, XPS, ToF-SIMS and Operando-QMS show the degrading effect an oxygen plasma has on PTFE. Even

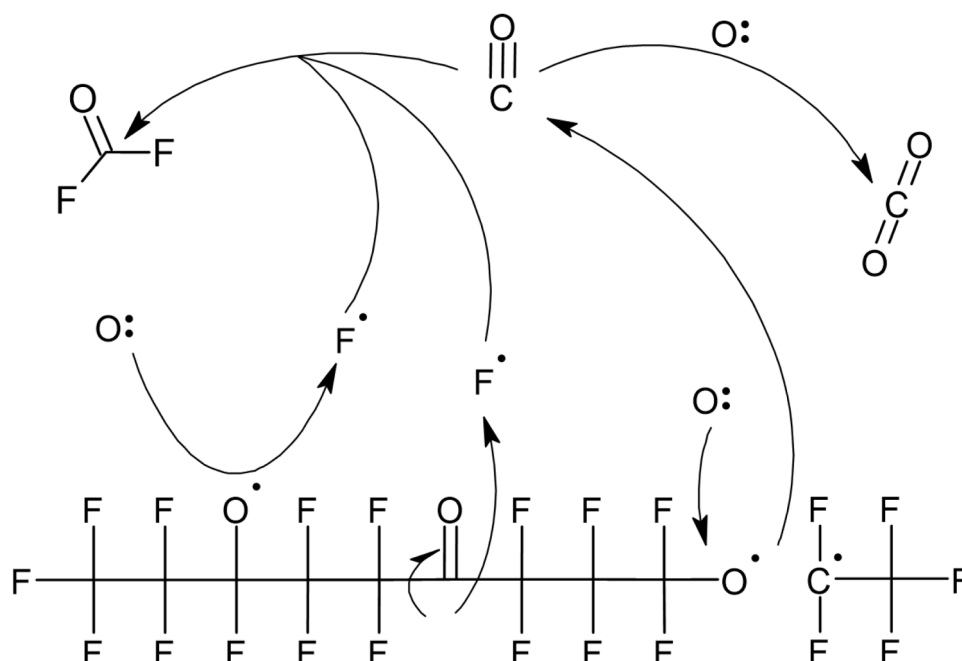


Fig. 9. Possible reaction scheme of the degradation occurring at the surface of PTFE with AO, as derived from surface analysis as well as operando mass spectrometry.

though the goal of the conducted experiments was to understand the long-term degradation of PTFE in an oxygen plasma, we were unable to replicate studies that showed harsh changes in surface composition after very short treatment times: Even though we also observed defluorination in XPS measurements, the change in fluorine content was not as strong as observed by Vandencastele et al. [18], who reported a steadily declining fluorine content down to 36 % after 20 min of oxygen plasma treatment. Neither were we able to reproduce the observation by Morra et al. [16], who found that the fluorine content decreases within seconds after plasma ignition to 50 % and then rises back up to 61.4 % after 15 min. These differences might be attributable to a different plasma setup. Also, it is unclear whether the entire surface of the samples in literature had been degraded by the plasma. This point is especially relevant, as within the first hours of plasma treatment we found a heterogeneous distribution of degradation on the surface. Nonetheless, we were able to use QMS to observe the presence of CO, CO₂⁺ and F in the plasma, as reported by Vandencastele et al. [18], who used optical emission spectroscopy to detect these fragments.

While the exact degradation mechanism likely is highly complex and involves many different reactions, the following statements can be made:

- After 2–4 h of plasma treatment, the entire surface is degraded. This time corresponds to a fluence of approximately 2.5–5 mmol AO·cm⁻², or 174–348 days in the LEO at a constant flux of 10¹⁴ atoms·cm⁻². For longer plasma durations, a quasi-equilibrium is reached, where degradation is occurring at the same rate as before, however no changes in surface composition can be observed.
- The degradation process involves the stripping of fluorine from the carbon chain, as is evident from the reduced fluorine content measured in XPS, increased presence of defluorinated carbon species in ToF-SIMS, as well as the presence of F⁺ during plasma conditions in QMS spectra.
- The slower degradation rate of PTFE in LEO compared to other, carbon chain based, polymers [10] indicates that the defluorination is the rate determining step in the degradation process.
- This defluorination likely results either in a bond between the defluorinated carbon atom and oxygen, or in a breaking of the

carbon chain. This can be deduced from the decrease in fluorinated carbon atoms in XPS that matches the increase of oxygenated and terminated carbon.

- Once the first fluorine atom is removed from a carbon, the second fluorine is likely much more reactive, as no evidence of single fluorinated carbon was found in XPS.
- After the complete defluorination, the carbon atom breaks apart from the polymer chain and can be detected as either C⁺ or oxygenated carbon, such as CO₂⁺ in QMS measurements. Note that defluorination appears to not be necessary for the carbon atom to be ablated from the sample, as a mass signal could be attributed to carbonyl fluoride (COF₂), indicating that not every carbon atom removed from the sample is defluorinated beforehand. As no carbon fragment with a single fluorine atom was visible in QMS measurements, either complete or no defluorination appears to be the condition for carbon ablation from the sample.
- During the degradation process, the average polymer chain length at the surface of the sample decreases. This can be deduced from the increase in terminated carbon atoms visible in XPS, as well as from the increasing significance of shorter carbon chains in the loadings obtained from MCR on ToF-SIMS surface spectra.
- By combining these deductions, a simplified reaction scheme can be constructed, as seen in Fig. 9.

5. Conclusion

ToF-SIMS, XPS, SEM and operando-MS measurements were employed to investigate the degradation of PTFE in a low-temperature oxygen plasma. It was found that the surface undergoes significant changes within the first 4 h of plasma treatment, corresponding to a dose of 2.5–5 mmol atomic oxygen·cm⁻². Samples treated for longer durations exhibited no further changes in surface composition. A steady loss of mass was noted during the experiments, remaining linear even for extended treatment times. The degradation is likely taking place by stripping the fluorine from a carbon atom and subsequent ablation of the (oxygenated) carbon atom from the surface, breaking the polymer chain apart, resulting in an increase of both defluorinated and terminated carbon atoms, as well as overall shorter carbon chains. Significant

indicators of degradation are an increase in terminated carbon chains, verified by XPS, ToF-SIMS and mass spectrometric in operando measurements. At the same time, the bulk material remained unaffected by the plasma treatment.

CRedit authorship contribution statement

Tobias Wagner: Writing – original draft, Visualization, Validation, Investigation, Data curation. **Marcus Rohnke:** Writing – review & editing, Project administration, Methodology, Conceptualization. **Jürgen Janek:** Writing – review & editing, Supervision, Funding acquisition, Conceptualization.

Declaration of competing interest

The authors declare the following financial interests/personal relationships which may be considered as potential competing interests:

Juergen Janek reports financial support by European Commission and article publishing charges were provided by German Research Foundation. If there are other authors, they declare that they have no known competing financial interests or personal relationships that could have appeared to influence the work reported in this paper.

Data availability

Data will be made available on reasonable request.

Acknowledgements

Financial support by the European Union (IWB EFRE program) under project no FPG991 003/2019 is gratefully acknowledged. The authors thank also the German Federal Ministry for Education and Research (BMBF) for funding the PHI Versa Probe 4 and the M6 Plus SIMS (project PROGRAL, no 03XP0427) as well as the German Research Foundation (DFG) for funding the Hybrid-SIMS under grant number INST 162/544–1 FUGG.

Supplementary materials

Supplementary material associated with this article can be found, in the online version, at [doi:10.1016/j.polyimdegradstab.2024.110989](https://doi.org/10.1016/j.polyimdegradstab.2024.110989).

References

- [1] I. Gouzman, E. Grossman, R. Verker, N. Atar, A. Bolker, N. Eliaz, *Advanced Materials* (Deerfield Beach, Fla.), 31, 2019 e1807738.
- [2] K.K. de Groh, B.A. Banks, S.K.R. Miller, J.A. Dever, *Handbook of environmental degradation of materials* (Third Edition) Chapter 28, Degradation of Spacecraft Materials (2018).
- [3] J. Chen, N. Ding, Z. Li, W. Wang, *Prog. Aerosp. Sci.* 83 (2016) 37, <https://doi.org/10.1016/j.paerosci.2016.02.002>.
- [4] X.-H. Zhao, Z.-G. Shen, Y.-S. Xing, S.-L. Ma, *Polym. Degrad. Stab.* 88 (2005) 275, <https://doi.org/10.1016/j.polyimdegradstab.2004.11.002>.
- [5] S. Abou Rich, P. Leroy, T. Dufour, N. Wehbe, L. Houssiau, F. Reniers, *Surf. Interface Anal.* 46 (2014) 164, <https://doi.org/10.1002/sia.5403>.
- [6] Z. Shpilman, I. Gouzman, G. Lempert, E. Grossman, A. Hoffman, *Rev. Sci. Instrum.* 79 (2008) 25106, <https://doi.org/10.1063/1.2885044>.
- [7] Y. Huang, X. Tian, S. Yang, P.K. Chu, *Rev. Sci. Instrum.* 78 (2007) 103301, <https://doi.org/10.1063/1.2800766>.
- [8] Z. Hooshangi, S.A. Hossein Feghhi, R. Saeedzadeh, *Acta Astronaut.* 119 (2016) 233, <https://doi.org/10.1016/j.actaastro.2015.11.031>.
- [9] T. Ghidini, *Nat. Mater.* 17 (2018) 846, <https://doi.org/10.1038/s41563-018-0184-4>.
- [10] K.K.de Groh, B.A. Banks, *Atomic Oxygen Erosion Data From the MISSE 2–8 Missions*, 2019.
- [11] E.M. Silverman, *Space Environ. Effects on Spacecraft: LEO Mater. Select. Guide* (1995).
- [12] S. Zanini, R. Barni, R.D. Pergola, C. Riccardi, *J. Phys. D: Appl. Phys.* 47 (2014) 325202, <https://doi.org/10.1088/0022-3727/47/32/325202>.
- [13] C. Liu, R.D. Arnell, A.R. Gibbons, S.M. Green, L. Ren, J. Tong, *Surf. Eng.* 16 (2013) 215, <https://doi.org/10.1179/026708400101517161>.
- [14] R. Zaplotnik, A. Vesel, M. Mozetič, *Plasma Process Polym* 15 (2018) 1800021, <https://doi.org/10.1002/ppap.201800021>.
- [15] Y. Gudimenko, R. Ng, J.I. Kleiman, Z.A. Iskanderova, R.C. Tennyson, P.C. Hughes, *Polymer Surface Modificat.: Relevance to Adhesion* (2004) 325, <https://doi.org/10.1201/b12183-18>.
- [16] M. Morra, E. Occhiello, F. Garbassi, *Surf. Interface Anal.* 16 (1990) 412, <https://doi.org/10.1002/sia.740160186>.
- [17] A.A.-G.A. Atta, *Indian J. Pure & Appl. Phys.* (2016) 551.
- [18] N. Vandencastele, D. Merche, F. Reniers, *Surf. Interface Anal.* 38 (2006) 526, <https://doi.org/10.1002/sia.2255>.
- [19] A. Vesel, M. Mozetic, A. Zalar, *Surf. Interface Anal.* 40 (2008) 661, <https://doi.org/10.1002/sia.2691>.
- [20] D. Heller, B. Hagenhoff, C. Engelhard, *Journal of Vacuum Science & Technology B, Nanotechnology and Microelectronics: Materials, Processing, Measurement, and Phenomena* 34 (2016) 49, <https://doi.org/10.1116/1.4948371>.
- [21] F. Awaja, J.B. Moon, M. Gilbert, S. Zhang, C.G. Kim, P.J. Pigram, *Polym. Degrad. Stab.* 96 (2011) 1301, <https://doi.org/10.1016/j.polyimdegradstab.2011.04.001>.
- [22] W.H. Lawton, E.A. Sylvestre, *Technometrics* 13 (1971) 617, <https://doi.org/10.1080/00401706.1971.10488823>.
- [23] A. de Juan, J. Jaumot, R. Tauler, *Anal. Methods* 6 (2014) 4964, <https://doi.org/10.1039/C4AY00571F>.
- [24] M.A. Lieberman, A.J. Lichtenberg, *Principles of Plasma Discharges and Materials Processing*, Wiley-Interscience, Hoboken, 2005.